Far-infrared and transport properties of antidot arrays with broken symmetry

A. Lorke[a],*, S. Wimmer[a], B. Jager[a], J.P. Kotthaus[a], W. Wegscheider[b], M. Bichler[b]

[a] *Sektion Physik, LMU München, Geschw.-Scholl-Pl. 1, 80539 München, Germany*
[b] *Walter Schottky Institut, TU München, Am Coulombwall, 85748 München, Germany*

Abstract

We investigate the high- and low-frequency magnetotransport of a square antidot lattice with a triangular basis. In the longitudinal magnetoresistance $\rho_{xx}(B)$ we observe higher-order commensurability features which reflect skipping orbits along the straight edges of the antidots. A magnetic field asymmetry in the four-probe resistance along the y-direction allows us to test basic symmetry relations in the transport coefficients. Under far-infrared irradiation the broken symmetry of the antidot array leads to a lateral photo-voltage which is attributed to a lateral, ratchet-type mechanism. © 1998 Elsevier Science B.V. All rights reserved.

Keywords: Antidot arrays; Commensurability effects; Broken symmetry

Two-dimensional electron gases with appropriately placed sub-micron voids are commonly called "antidot arrays". In these systems, the interplay between electric and magnetic forces leads to a number of novel effects both in the high- and low-frequency transport properties [1–6]. Even though these transport properties have recently been investigated in great detail, most studies so far have been carried out in the linear regime. In this regime, the applied bias is a negligible perturbation, so that the experimentally determined quantities reflect equilibrium properties of the electron system. Then the Einstein relation, the Kubo formula and the Landauer–Büttiker formalism can be used very success-

fully for a theoretical treatment [7,8] and experimentally, the Onsager–Casimir symmetry relations [9,10] are expected to hold.

Here, we investigate the transport properties of antidot arrays with a broken reflection symmetry. By studying the influence of current and magnetic field reversal on the measured transport coefficients, we directly obtain information on the validity of the Onsager–Casimir relations in low-frequency transport. Furthermore, we investigate the response of such structures in the far-infrared regime and find a lateral photo-voltage which suggests that the high-frequency excitation, together with the broken symmetry leads to a net lateral charge transport.

The antidot arrays are fabricated on shallow high electron mobility transistor structures grown

* Corresponding auhor. Fax: + 49 89 2180 3182; e-mail: axel.lorke@physik.uni-muenchen.de.

by molecular-beam epitaxy on semi-insulating GaAs substrate. The active layers of the hetero-structure are as follows: 1 μm GaAs, 20 nm AlGaAs spacer, Si δ-doping layer, 2 nm GaAs, 2 nm AlAs, 8 nm AlGaAs and 5 nm GaAs cap. In unpatterned samples the electron density and mobility are 3.3×10^{11} cm^{-2} and 2.4×10^{5} cm^2/V s. The small distance between the heterointerface and the sample surface of only $d = 37$ nm is necessary to transfer the lithographically defined patterns into the two-dimensional electron gas without blurring the fine feature of the antidot shape. This is essential for our structures which deviate from the usual round or elliptic symmetry.

Using standard photolithographic techniques, a Hall bar is defined by wet etching and provided with alloyed AuGe Ohmic contacts. The antidot pattern is generated by electron beam lithography and shallow wet etching. Fig. 1a displays an atomic force micrograph of the resulting surface pattern, which consists of triangular antidots on a *square* lattice. The period of the lateral super-lattice is $a = 500$ nm, the triangles have a nominal base width of 300 nm and a height of 200 nm.

In Fig. 1a–c, schematic representations are shown of how the symmetry properties of the anti-dot array might affect ballistic electron trajectories. As shown in Fig. 1a, electrons which are ejected through the narrow constrictions between antidots will be collimated into the constriction of the ad-jacent antidot row only for one bias direction. For the opposite bias such collimation is absent and a larger fraction of the electrons will be reflected back into the emitter region. In magnetic fields, the low-frequency transport is affected by "runaway trajectories" [11,12] when the cyclotron diameter equals the lattice period, $2R_c = a$, as shown in Fig. 1b. In the present lattice, runaway trajectories in one direction are guided by the straight bound-aries on one side of the antidot rows, whereas they are scrambled by the zig-zag potential on the oppo-site side. Similar considerations apply to the elec-tron focusing trajectories shown in Fig. 1c. Note that while case (a) is in violation of the On-sager–Casimir relation, cases (b) and (c) are not. Fig. 1d schematically displays a further mechanism which is present in superlattices with broken sym-metry. On a path along the x-direction, an electron will experience a gradual increase of the potential, as the constriction between the antidots narrows. As it passes through the narrowest part of the tapered constriction, it experiences a more sudden potential drop. Thus, in this adiabatic picture, the motion along x is influenced by an asymmetric "saw-tooth" potential. For high-frequency excita-tion the combination of the saw-tooth potential and the sloshing motion of the electrons is expected to lead to a net current along the x-direction, similar to the motion of a harmonically driven ratchet [13].

For the experimental observation of the above mechanisms, an important question is whether the potential experienced by the electrons matches the pattern on the sample surface, or whether the fine features of the pattern are washed out due to screening and the distance between the 2DEG and the surface. Fig. 2 shows the longitudinal mag-neto-resistance $\rho_{xx}(B)$ at $T = 4.2$ K and a constant current of $I = 1$ μA. At low magnetic fields the resistance is increased by more than an order of magnitude with respect to the unpatterned part of the sample. At high magnetic fields (>4 T, not shown here) both resistances are in agreement with-in $\approx 20\%$ and the positions of the Shubnikov–de Haas minima are identical within a few percent. This shows that the areas between the antidots are only little affected by the patterning and that the potential drops off rapidly in the vicinity of the antidots. At $|B| = 0.4$ T (upward pointing arrows)
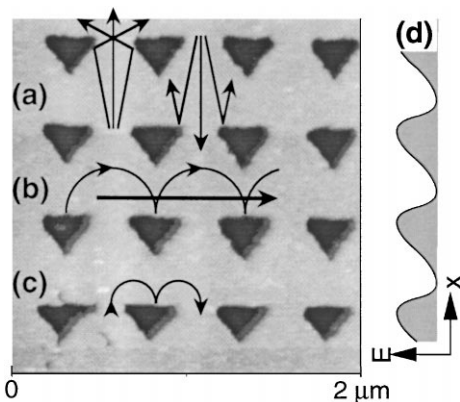

Fig. 1. (a)–(c) Atomic force micrograph of the etched antidot lattice and relevant electron trajectories. (d) Saw-tooth potential caused by the triangular antidots.
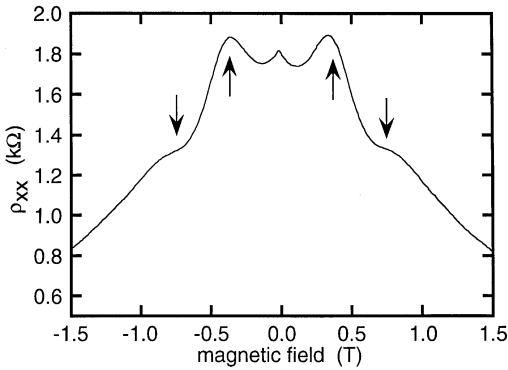
Fig. 2. Longitudinal resistance as a function of magnetic field. Commensurability features for both $2R_c \approx a$ (↑) and $2R_c \approx a/2$ (↓) are observed.

Fig. 3. Voltage signals as a function of magnetic field for different four-probe measurement configurations.

a maximum is observed in ρ_{xx}, which is identified as the well-known commensurability peak, commonly observed in antidot arrays at magnetic fields where the cyclotron diameter $2R_c$ equals the superlattice period a [1,3]. We observe no peaks at lower magnetic fields which would correspond to orbits around multiple antidots [14,15], since such orbits are geometrically not possible for the given pattern. However, we observe an additional structure in ρ_{xx} at $|B| = 0.8$ T (downward pointing arrow) which corresponds to the condition $2R_c \approx a/2$. We identify this structure with skipping orbits as shown in Fig. 1c. Even though these skipping orbits are well known from the electron-focusing experiments, to the best of our knowledge, this is the first observation of such "fractional" commensurabilities in two-dimensional arrays of antidots. After illuminating the sample, both peaks are shifted towards higher magnetic fields in agreement with the increased carrier density, which shows that the commensurability condition $2R_c = a/2$ observed in Fig. 2 is not coincidental. Since the presence of higher-order skipping orbits requires straight edges, we conclude that the triangular surface pattern has been transferred into the 2DEG with sufficient accuracy.

Within the accuracy of the experiment, no difference is observed between $\rho_{xx}(B)$ and $\rho_{xx}(-B)$. This is in agreement with the fact that the lattice is symmetric with respect to a 180° rotation around the x-axis [16].
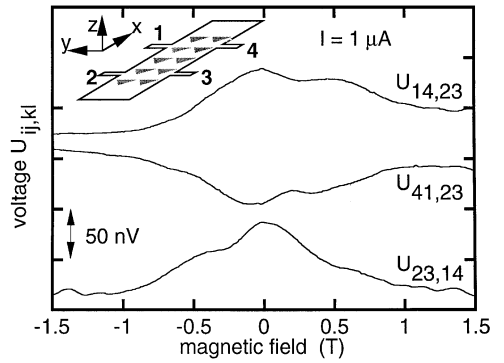
A different behavior is observed for the resistance *across* the Hall bar. In Fig. 3, the measured voltage $U_{ij,kl}$ for a bias of $|I| = 1$ µA is shown for a number of measurement configurations. Using the notation of the inset, the first two indices correspond to the current leads, the second to the voltage probes. The traces in Fig. 3 have been offset for clarity and to compensate for thermal voltages. Before discussing the curves in more detail, let us summarize the most relevant symmetry properties in the transport coefficients for the present geometry.

$$U_{14,23}(B) = U_{23,14}(-B), \qquad (1)$$

$$U_{14,23}(B) = -U_{41,23}(B), \qquad (2)$$

$$U_{14,23}(B) = U_{32,41}(B). \qquad (3)$$

The first identity represents the Onsager–Casimir relation. The second corresponds to the fact that the voltage will reverse when the current is reversed. (Eqs. (1) and (2) are closely related and Eq. (2) can easily be derived from Eq. (1)). The third identity follows from a rotation of 180° around the z-axis and holds for common, rotationally or 4-fold symmetric antidots on a square or rectangular lattice. Note that also a possible tilt of the Hallbar with respect to the lattice should not affect this symmetry. From all three identities follows that the longitudinal resistance is symmetric with respect to the inversion of the magnetic field, $U_{14,23}(B) = U_{14,23}(-B)$. This is clearly not the case in the given

structure, as seen in Fig. 3, where the commensurability peak at $|B| \approx 0.4$ T is much better resolved for positive magnetic fields than for negative. This is not a consequence of possible nonlinear transport, as seen from a comparison between $U_{14,23}$ and $U_{41,23}$. Within the accuracy of the experiment we find $U_{14,23} = -U_{41,23}$, in agreement with relation (2). Furthermore, a comparison between $U_{14,23}$ and $U_{23,14}$ shows that the Onsager–Casimir relation holds (Eq. (1)). We thus conclude that the observed asymmetry in $U_{ij,kl}$ is a consequence of the violation of the symmetry of the lattice (Eq. (3)), which is a further confirmation for the triangular shape of the antidots.

The experimental results shown in Figs. 2 and 3 are not affected by mechanisms such as shown in Fig. 1a which would violate the current reversal symmetry, Eq. (2). For the present samples, Eq. (2) holds for a wide range of experimental conditions with currents up to 100 μA. However, for single, asymmetric antidots embedded in a cross-junction which allows for a much better controlled injection of ballistic electrons, a "ballistic rectification", similar to that shown in Fig. 1b has recently been observed [17].

To investigate the response of the antidot lattice to high-frequency excitation, the sample is illuminated by modulated far-infrared radiation of 119 μm wavelength and a few mW power. The lateral photovoltage is recorded using a standard lock-in technique. No external bias or current is applied to the sample.

Fig. 4 displays the lateral photovoltage U_{phot} between source and drain as a function of the magnetic field. For comparison, the longitudinal resistance $\rho_{xx}(B)$ is plotted as well (right scale). Despite the poor signal-to-noise ratio, a clear positive photovoltage, induced by the far-infrared irradiation is observed. A number of observations strongly support the conjecture that this photosignal is caused by the anisotropy of the antidot lattice rather than by spurious effects such as inhomogeneous illumination or irradiation of the Ohmic contacts: The magnetic-field dependence of the photo-signal closely follows the commensurability features in the longitudinal resistance. This is not simply an effect of the fluctuating resistance of the antidot lattice, together with a spurious photo-
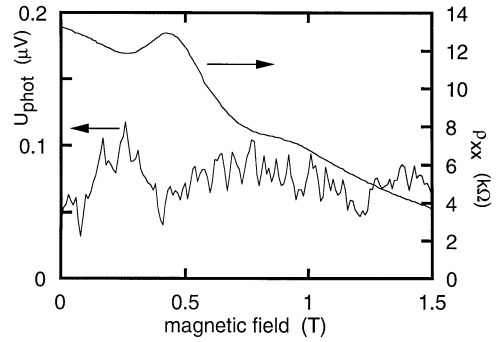

Fig. 4. Lateral photovoltage induced by far-infrared irradiation. For comparison, the lateral magnetoresistivity is also given.

current, since maxima in ρ_{xx} correspond to minima in the photo-signal. Furthermore, U_{phot} changes by a much larger fraction (almost 50%) and does not reflect the gradual decrease of ρ_{xx} with magnetic field. Most importantly, the direction of the photovoltage is in agreement with the picture of the saw-tooth potential outlined above. We therefore attribute the lateral photo-voltage to the rectification of the THz frequency by the broken symmetry of the antidot pattern. At present, the exact mechanism that leads to this rectification is not completely understood. An analysis of this effect requires a detailed treatment of the collective response of the electron system to the antidot potential and the far-infrared radiation and is beyond the scope of this paper.

In conclusion, we have investigated the low- and high-frequency response of a square antidot lattice with a triangular basis. In DC-transport, the triangular shape, with its straight edges, made possible the observation of a new class of skipping-orbit trajectories, which are absent in the commonly used circular geometry. Furthermore, the broken symmetry of the antidot lattice allowed us to investigate the validity of the Onsager–Kasimir relation in complex, mesoscopic structures. Under high-frequency excitation the antidot lattice exhibits a lateral photovoltage which in a magnetic field is influenced by commensurability effects. In a simple picture, this lateral photo-signal can be understood as a consequence of sloshing electrons in a saw-tooth potential which leads to a net

current of electrons along the symmetry axis of the antidot lattice.

References

[1] A. Lorke et al., Superlattices and Microstructures 9 (1991) 103.
[2] A. Lorke et al., Phys. Rev. B 44 (1991) 3447.
[3] K. Ensslin, P.M. Petroff, Phys. Rev. B 41 (1990) 12307.
[4] D. Weiss et al., Phys. Rev. Lett. 66 (1991) 2790.
[5] K. Kern et al., Phys. Rev. Lett. 66 (1991) 1618.
[6] E. Vasiliadou et al., Phys. Rev. B 52 (1995) R8658.
[7] Fleischmann et al., Phys. Rev. Lett. 68 (1992) 1367.
[8] Fleischmann et al., Europhys. Lett. 25 (1994) 219.
[9] M. Büttiker, Phys. Rev. Lett. 57 (1986) 1761.
[10] M. Büttiker, Phys. Rev. B 38 (1988) 9375.
[11] E.M. Baskin et al., JETP Lett 55 (1994) 679.
[12] R. Schuster et al., Phys. Rev. B 50 (1994) 8090.
[13] see, e.g., P. Reimann et al., Phys. Rev. Lett. 79 (1997) 10 and references therein.
[14] K. Nakamura et al., Superlattices Microstruct. 9 (1991) 235.
[15] S. Lüthi et al., Phys. Rev. B 55 (1997) 13088.
[16] Note, however, that both an unintentional tilt of the Hallbar with respect to the lattice and a possible difference in the properties of the edges might break this symmetry.
[17] A. Song et al., Phys. Rev. Lett., accepted.